



HAL
open science

Refined Asymptotic Approximations for the Phase Plane Trajectories of the SIR Model with Vital Dynamics

Todd L Parsons, David J D Earn

► **To cite this version:**

Todd L Parsons, David J D Earn. Refined Asymptotic Approximations for the Phase Plane Trajectories of the SIR Model with Vital Dynamics. 2023. hal-04178983

HAL Id: hal-04178983

<https://cnrs.hal.science/hal-04178983v1>

Preprint submitted on 8 Aug 2023

HAL is a multi-disciplinary open access archive for the deposit and dissemination of scientific research documents, whether they are published or not. The documents may come from teaching and research institutions in France or abroad, or from public or private research centers.

L'archive ouverte pluridisciplinaire **HAL**, est destinée au dépôt et à la diffusion de documents scientifiques de niveau recherche, publiés ou non, émanant des établissements d'enseignement et de recherche français ou étrangers, des laboratoires publics ou privés.

Refined Asymptotic Approximations for the Phase Plane Trajectories of the SIR Model with Vital Dynamics

Todd L. Parsons¹ and David J. D. Earn²

¹Laboratoire de Probabilités, Statistique et Modélisation (LPSM), Sorbonne Université, CNRS UMR 8001, Paris, France, 75005

²Department of Mathematics and Statistics, McMaster University, Hamilton, Ontario, Canada, L8S 4K1

August 8, 2023 @ 18:35

Abstract

We build on our previous work to derive more accurate analytical approximations for the phase-plane trajectories of the standard susceptible-infectious-removed (SIR) epidemic model, including host births and deaths. From our refined analysis, we obtain closed-form analytical expressions for the maximum and minimum prevalence following an initial outbreak. As in our previous work, our analysis involves matching asymptotic expansions across branch cuts of the Lambert W function, but we carry the approximations to higher asymptotic orders.

1 Introduction

In 1927, Kermack and McKendrick [5] (hereafter KM) published the system of ordinary differential equations (ODEs) that are now known as the standard susceptible-infectious-removed (SIR) model,

$$\frac{dX}{dt} = \mu(1 - X) - \beta XY, \quad (1a)$$

$$\frac{dY}{dt} = (\beta X - \gamma - \mu)Y, \quad (1b)$$

$$\frac{dZ}{dt} = \gamma Y - \mu Z. \quad (1c)$$

Here, the state variables are the proportions of the population that are susceptible (X), infective (Y), and removed (Z), and the parameters are the *per capita* rate of birth and death (μ), the transmission rate (β), and the recovery (or removal) rate (γ). Since $X + Y + Z = 1$, the dynamical system (1) is two-dimensional. KM found the exact solution in the phase plane in the absence of vital dynamics ($\mu = 0$), but no exact solution is known for $\mu > 0$.

In a previous paper [10], we used multiple scale and singular perturbation methods [8, 6] to obtain closed-form analytical approximations to the phase-plane trajectories of Equation (1) in the presence of host births and deaths ($\mu > 0$). Here, we extend our analyses to higher order and obtain more accurate trajectory approximations.

As in our lower order analysis [10], the small parameter¹ we use for perturbation expansions is

$$\epsilon = \frac{\epsilon}{\mathcal{R}_0}, \quad (2)$$

Key words and phrases. epidemics, SIR model, matched asymptotics, Poincaré map.

1991 *Mathematics subject classification.* 34E05, 34E13, 37N25, 92D30

¹See [10, Table 1] for parameter estimates for common infectious diseases. Typically $\epsilon < 0.001$.

25 where ε is the expected infectious period $[1/(\gamma + \mu)]$ in units of the expected host lifetime $(1/\mu)$, and \mathcal{R}_0 is
 26 the basic reproduction number $[\beta/(\gamma + \mu)]$. The endemic equilibrium (EE) of the SIR ODEs (1) is

$$27 \quad x_* = \frac{1}{\mathcal{R}_0}, \quad y_* = \varepsilon(1 - x_*). \quad (3)$$

28 If we express time in units of the expected infectious period $[\tau = t(\gamma + \mu)]$, then Equation (1) can be
 29 conveniently written

$$30 \quad x_* \frac{dX}{d\tau} = \varepsilon(1 - X) - XY, \quad (4a)$$

$$31 \quad x_* \frac{dY}{d\tau} = (X - x_*)Y, \quad (4b)$$

32 so the phase plane equation can be written

$$\frac{dY}{dx} = \frac{(x - x_*)Y}{\varepsilon(1 - x) - xY} \quad \text{or} \quad \frac{dX}{dy} = \frac{\varepsilon(1 - X) - Xy}{(X - x_*)y}. \quad (5)$$

33 As in [10], we use the probabilist’s convention that lower case letters indicate independent variables and
 34 capitals indicate dependent variables.

35 Our previous approximation [10] is “zeroth order” in the sense that it is based on matching asymptotic
 36 expansions to KM’s phase plane solution to Equation (5) for $\varepsilon = 0$ (which is a good approximation away
 37 from the coordinate axes if $0 < \varepsilon \ll 1$). The approximation we present here is “first order” in the sense that
 38 it is based on matching to an $\mathcal{O}(\varepsilon)$ correction to KM’s exact solution for $\varepsilon = 0$. We put these labels in quotes
 39 because they do not reflect the ultimate asymptotic orders of the approximations we have derived.

40 Our “zeroth order” approximation yields an analytical formula for the proportion susceptible near the
 41 end of a major outbreak, which is an important component of an analysis of epidemic burnout that we have
 42 conducted based on the stochastic SIR model [9]. Our “first order” approximation allows us to obtain an
 43 estimate of the burnout probability that does not require an *a priori* choice of boundary layer, which in turn
 44 allows us to show that the prior estimate of the burnout probability presented by van Herwaarden [11] can
 45 be derived as an approximation to our result in [9].

46 Like the approximations of van Herwaarden [11], our “first order” results depend on the numerical
 47 evaluation of integrals. However, we do obtain “integral free” inner solutions—*i.e.*, we obtain closed-form
 48 analytical results for the dynamics inside all boundary and corner layers—and are consequently able to derive
 49 convenient, closed-form “first order” expressions for the peak prevalence and the minimum prevalence after
 50 the first major epidemic following disease invasion.

51 As in our “zeroth order” analysis, we succeed in obtaining a “first order” approximation that is valid to
 52 the same order in ε throughout the phase plane. Critical ingredients in our approach are the use of Lambert’s
 53 W function [3] to invert implicit relations, and matching across branch cuts of the W function.

54 A much more detailed introduction to the SIR model and the method of asymptotic matching is given
 55 in our previous paper [10]. Our new results are summarized in Table 3.

56 2 Prior Work

57 In Table 1, we summarize the approximate solutions to Equation (4) that we constructed in [10]; each of
 58 these **local solutions** is valid only in a subset of the phase-plane. The **outer solution**, obtained in [10] by
 59 assuming an asymptotic series in powers of ε ,

$$Y^{\text{out}}(x; \varepsilon) = \sum_{j=0}^{\infty} Y_j^{\text{out}}(x) \varepsilon^j, \quad (6)$$

60 and neglecting terms of $\mathcal{O}(\varepsilon)$, captured the behaviour of the exact solution in the majority of phase space.

61 The x -axis **boundary layer** solution, obtained in [10] via a WKB ansatz [1, Chapter 10], is valid where y

62 is **transcendentally small**, *i.e.*, where y vanishes more rapidly than any power ϵ^j as $\epsilon \rightarrow 0$ [6, p. 4]. Finally,
63 we derived two **corner layer** solutions by assuming that $y = \mathcal{O}(\epsilon)$, which enabled us to smoothly match the
64 outer and boundary layer solutions. We combined these local solutions into a single **matched asymptotic**
65 **solution** approximating the trajectory of a novel pathogen invading at the **disease-free equilibrium**
66 (DFE, $(x_i, y_i) = (1, 0)$). This single solution was expressed as a multi-function in y , valid everywhere in
67 the phase-plane, with different branches giving the trajectories in the left and right half-planes ($x \leq x_*$ and
68 $x \geq x_*$).

Solution	Notation	Expression	Scaling
Outer	$\overset{\text{out}}{Y}_0(x)$	$\overset{\text{out}}{C}_0 - x + x_* \ln x$	$x = \mathcal{O}(1),$ $y = \mathcal{O}(1)$
Corner	$\overset{\text{cor}}{X}(y; \epsilon)$	$\overset{\text{cor}}{C}_0 + \left(\frac{\overset{\text{cor}}{C}_0}{x_* - \overset{\text{cor}}{C}_0} \right) y + \epsilon \ln \epsilon^{-1} \left(\overset{\text{cor}}{C}_{\ln} + \frac{1 - \overset{\text{cor}}{C}_0}{x_* - \overset{\text{cor}}{C}_0} \right) - \epsilon \left[\left(\frac{1 - \overset{\text{cor}}{C}_0}{x_* - \overset{\text{cor}}{C}_0} \right) \ln y - \overset{\text{cor}}{C}_1 \right]$	$x = \mathcal{O}(1),$ $y = \mathcal{O}(\epsilon)$
x -axis bdry	$\overset{\text{xb}}{Y}(x; \epsilon)$	$(1 - x)^{-\frac{1}{\epsilon}(1 - x_*)} e^{\frac{1}{\epsilon}(C_0^\phi - x) + C_1^\phi}$	$x = \mathcal{O}(1),$ $y = \text{TS}$

Table 1: Local solutions constructed in [10]. TS indicates a quantity that is transcendentally small. Throughout, we adopt the convention that C , with any combination of sub- and/or superscripts, indicates a constant of integration.

69 3 Refined Asymptotic Solutions

70 As the small parameter ϵ is increased, the outer solution $\overset{\text{out}}{Y}_0(x)$ [Table 1] becomes a progressively poorer
71 approximation to the first epidemic. As a consequence our subsequent corner and boundary layer approx-
72 imations – and thus the matched solution – also perform less well. To resolve this, here we seek a second
73 matching that includes the correction term $\overset{\text{out}}{Y}_1(x)$ (6), again focusing on the solution along the unstable
74 manifold, $x_i = 1$. Unlike our previous matching, where we expressed all local solutions as functions of y ,
75 we have not found a way to invert the relation $y = \overset{\text{out}}{Y}_1(x)$ that we obtain, so in this section we will match
76 functions of x .

77 These higher order corrections come at the cost of (considerably) complicating our analytical expressions.
78 In particular, we are obliged to introduce integrals that do not appear to have closed form solutions, and
79 which are numerically sensitive due to singular terms in the integrand. In Appendix A we obtain some
80 analytical approximations to these integrals by other means (the integrals are independent of ϵ , so we cannot
81 use our matched asymptotic approach). Furthermore, for any given value of \mathcal{R}_0 , fully matched solutions are
82 available only for sufficiently small ϵ (see Appendix B for the \mathcal{R}_0 -dependent condition on ϵ ; we remark that
83 even when this condition is violated, the outer and boundary layer solutions continue to provide excellent
84 local approximations).

85 3.1 The KM Solution

86 Given an initial condition (x_i, y_i) , the constant of integration in $\overset{\text{out}}{Y}_0(x)$ is readily found to be

$$\overset{\text{out}}{C}_0 = y_i + x_i - x_* \ln x_i, \quad (7)$$

87 so that

$$87 \quad Y_0^{\text{out}}(x, x_i, y_i) = y_i + x_i - x + x_* \ln\left(\frac{x}{x_i}\right), \quad (8)$$

88 which is the phase plane solution first discovered by KM for the SIR ODEs without vital dynamics, *i.e.*, for
89 $\epsilon = 0$.

90 Provided $x_i \geq x_*$ and $y_i \geq 0$, the solution (8) is non-negative and concave, with two positive roots,

$$x_f(x_i, y_i) = -x_* W_0\left(\mathcal{E}(-x_i/x_*) e^{-\frac{y_i}{x_*}}\right). \quad (9)$$

91 in $(0, x_*)$, and another in $(x_*, 1)$, and a unique maximum \bar{y}_0 at x_* ,

$$\bar{y}_0(x_i, y_i) = Y_0^{\text{out}}(x_*, x_i, y_i) = y_i + x_i - x_* (1 + \ln(x_i/x_*)). \quad (10)$$

92 Here, W_0 denotes the principal branch of the Lambert W -function²

93 $\bar{y}_0(x_i, y_i)$ and $x_f(x_i, y_i)$ are the true peak prevalence and final size for the SIR model without vital dynam-
94 ics ($\epsilon = 0$) started from (x_i, y_i) . \bar{y}_0 only approximates the peak prevalence for the model with demography,
95 and there is no “final” size if there is a continuous inflow of new susceptible individuals. Nevertheless, we
96 informally refer to x_f as the “final size” for convenience. Moreover, when there is no risk of confusion, for
97 ease of notation we will write $x_f(x_i, 0) = x_f(x_i)$ and $x_f(1, 0) = x_f$ and similarly for \bar{y}_0 .

98 As in [10], our ultimate goal is to approximate the solution corresponding to invasion at the DFE,
99 $(x_i, y_i) = (1, 0)$, but in order to obtain matched asymptotic approximations that continue into the second
100 and subsequent epidemic waves, we need to consider solutions for more general initial conditions. In [10] we
101 derived **effective initial conditions** $(x_{i,2}, 0)$ that allow us to approximate these waves. Given an initial
102 condition (x_i, y_i) , we set

$$x_{i,2}(x_i, y_i) = 1 + (1 - x_*) W_0\left(\mathcal{E}\left(-\frac{1 - x_f(x_i, y_i)}{1 - x_*}\right)\right). \quad (12)$$

103 As we explained in [10], although $(x_{i,2}, 0)$ is not a point on the actual trajectory, it is an “effective” initial
104 condition for the second wave in the following sense: if $(x_{i,2}, 0)$ were used as the initial state in the KM
105 ($\epsilon = 0$) solution, the resulting trajectory would meet the second rise of the actual solution as it curves up
106 from the left in the phase plane.

107 3.2 The First Order Outer Solution

108 If we now include the second term in the asymptotic expansion (6),

$$Y(x; \epsilon) = Y_0^{\text{out}}(x) + \epsilon Y_1^{\text{out}}(x) + \mathcal{O}(\epsilon^2), \quad (13)$$

109 we must now solve for $Y_1^{\text{out}}(x)$, which, substituting (6) into Equation (4) and collecting $\mathcal{O}(\epsilon)$ terms, satisfies

$$\frac{dY_1^{\text{out}}}{dx} = \left(\frac{1}{x} - 1\right) \left(\frac{x_*}{x} - 1\right) \frac{1}{Y_0^{\text{out}}(x)}. \quad (14)$$

²If $\mathcal{E}(z) = ze^z$, Lambert’s W -function $W(z)$ [3] solves the “left-sided” inverse relation $\mathcal{E}(W(z)) = z$. This equation has countably many solutions, each corresponding to branches W_i of the W -function; we will need the two real branches, W_0 , which maps $[-\frac{1}{e}, \infty)$ to $[-1, \infty)$, and W_{-1} , which maps $[-\frac{1}{e}, 0)$ to $(-\infty, -1]$. For these two branches, W_i is a *partial* “right-sided” inverse function for $\mathcal{E}(z)$:

$$\begin{aligned} W_{-1}(\mathcal{E}(z)) &= z & \text{if } z \leq -1 \\ W_0(\mathcal{E}(z)) &= z & \text{if } z \geq -1. \end{aligned} \quad (11)$$

110 This equation can be formally solved by (indefinite) integration. If we impose the initial condition (x_i, y_i) ,
 111 the first order term, $Y_1^{\text{out}}(x)$, in the asymptotic series for the outer solution (6), takes the form

$$Y_1^{\text{out}}(x, x_i, y_i) = \int \left(\frac{1}{x} - 1\right) \left(\frac{x_*}{x} - 1\right) \frac{1}{Y_0^{\text{out}}(x, x_i, y_i)} dx. \quad (15)$$

112 This integral has no closed analytical form so we will need to evaluate it numerically. To do so, we must fix
 113 an endpoint to make it a definite integral, which requires some care: $Y_0^{\text{out}}(x, x_i, y_i)$ (8), which appears in the
 114 denominator of the integrand in Equation (15), vanishes at $x_f(x_i, y_i)$, and if $y_i = 0$ then $Y_0^{\text{out}}(x, x_i, y_i)$ vanishes
 115 at x_i as well. Consequently, there is a pair of possible singularities in the integrand. If $y_i = 0$ and $x_i = 1$
 116 then the integrand approaches x_* in the limit as $x \rightarrow 1$ and the singularity is removable. However, if $y_i = 0$
 117 then the integrand is singular for all $x_i \neq 1$. Moreover, the integrand is always singular at $x_f(x_i, y_i)$. Since
 118 we need to be able to compute $Y_1^{\text{out}}(x, x_i, y_i)$ at values of $x \in (x_f(x_i, y_i), x_i)$, we must choose an endpoint that
 119 lies in that interval as well. The natural choice is x_* , which always satisfies $x_f(x_i, y_i) < x_* < x_i$. For any
 120 $x \in (x_f, x_i)$, the integrand is then non-singular on $[x, x_*]$ ($[x_*, x]$) if $x < x_*$ (resp. $x > x_*$).

121 Since the specification of an arbitrary endpoint is just a device to be able to compute the integral (15)
 122 numerically, we must still include an arbitrary constant of integration, which will provide a degree of freedom
 123 that we will need when imposing initial conditions. Thus, we write

$$Y_1^{\text{out}}(x, x_i, y_i) = \int_{x_*}^x \left(\frac{1}{u} - 1\right) \left(\frac{x_*}{u} - 1\right) \frac{1}{Y_0^{\text{out}}(u, x_i, y_i)} du + C_1^{\text{out}}. \quad (16)$$

124 Henceforth, we will limit our attention to solutions with $y_i = 0$, which we denote by $Y_1^{\text{out}}(x, x_i)$. When
 125 focussing more specifically on the solution with $(x_i, y_i) = (1, 0)$, we will write simply $Y_1^{\text{out}}(x)$, but we do need
 126 the extra freedom of an arbitrary x_i to consider subsequent epidemic waves. For all such solutions $Y_1^{\text{out}}(x, x_i)$,
 127 the integrand in (16) has a simple pole at $x = x_f(x_i)$ (9) with residue

$$\lim_{x \rightarrow x_f(x_i)} (x - x_f(x_i)) \left(\frac{1}{x} - 1\right) \left(\frac{x_*}{x} - 1\right) \frac{1}{Y_0^{\text{out}}(x, x_i)} = \frac{1}{x_f(x_i)} - 1. \quad (17)$$

128 If $x_i \neq 1$, it also has a second simple pole at $x = x_i$ with residue $\frac{1}{x_i} - 1$. To be able to evaluate the integral
 129 (16), we shall need to remove these poles, separating the integral into singular and non-singular parts; doing
 130 so will also prove to be an essential step in matching the solutions.

131 Presentation of calculations will be greatly simplified by introducing the notation

$$\mathcal{Y}_a^b(x_i) = \int_a^b \left[\left(\frac{1}{u} - 1\right) \left(\frac{x_*}{u} - 1\right) \frac{1}{Y_0^{\text{out}}(u, x_i)} - \left(\frac{1}{x_i} - 1\right) \frac{1}{u - x_i} - \left(\frac{1}{x_f(x_i)} - 1\right) \frac{1}{u - x_f(x_i)} \right] du. \quad (18)$$

132 Here, the sub- and superscripts a and b are used to emphasize their role as endpoints of an integral, and in
 133 particular that

$$\mathcal{Y}_a^b(x_i) = \mathcal{Y}_a^c(x_i) + \mathcal{Y}_c^b(x_i), \quad \text{for any } c \in \mathbb{R}. \quad (19)$$

134 We can then re-write (16) as

$$\begin{aligned} Y_1^{\text{out}}(x, x_i) &= \mathcal{Y}_{x_*}^x(x_i) + \int_{x_*}^x \left(\frac{1}{x_i} - 1\right) \frac{1}{u - x_i} du + \int_{x_*}^x \left(\frac{1}{x_f(x_i)} - 1\right) \frac{1}{u - x_f(x_i)} du + C_1^{\text{out}} \\ &= \mathcal{Y}_{x_*}^x(x_i) + \left(\frac{1}{x_i} - 1\right) \ln \left(\frac{x_i - x}{x_i - x_*}\right) + \left(\frac{1}{x_f(x_i)} - 1\right) \ln \left(\frac{x - x_f(x_i)}{x_* - x_f(x_i)}\right) + C_1^{\text{out}}. \end{aligned} \quad (20)$$

135 The first order approximation to the outer solution is thus

$$Y^{\text{out}}(x, x_i; \epsilon) = Y_0^{\text{out}}(x, x_i) + \epsilon Y_1^{\text{out}}(x, x_i). \quad (21)$$

136 Note that when $x_i = 1$, which is our focal solution, all terms in Equations (18) and (20) involving the residue
 137 $\frac{1}{x_i} - 1$ vanish; in what follows we will write $Y(x, 1; \epsilon)$ as $Y(x; \epsilon)$.

138 **Analytical matching** In general, $\mathcal{Y}_{x_*}^x(x_i)$ can only be computed numerically, so our first order solution is
 139 only semi-analytical. In the limit where \mathcal{R}_0 is near 1, however, we show in Appendix A that a satisfactory
 140 analytical approximation to $\mathcal{Y}_{x_*}^x(x_i)$ can be found, which enables us to give a fully-analytical first order
 141 matched solution.

142 3.2.1 Outer solution from the DFE

143 Specializing now to the case $(x_i, y_i) = (1, 0)$, we must have $Y(1) = 0$. Since $Y_0^{\text{out}}(1) = 0$ [Equation (8)], to retain
 144 the correct initial condition we must have $Y_1^{\text{out}}(1) = 0$ also; hence from Equation (20) we infer that

$$145 \quad C_1^{\text{out}} = -\mathcal{Y}_{x_*}^1(1) - \left(\frac{1}{x_f} - 1\right) \ln\left(\frac{1 - x_f}{x_* - x_f}\right), \quad (22)$$

whence

$$146 \quad Y(x; \epsilon) = Y_0^{\text{out}}(x) + \epsilon \left(\left(\frac{1}{x_f} - 1\right) \ln\left(\frac{x - x_f}{1 - x_f}\right) - \mathcal{Y}_x^1(1) \right). \quad (23)$$

146 **Peak prevalence** We obtain an approximation to \bar{y} by evaluating Equation (23) at $x = x_*$, which yields

$$147 \quad \bar{y}_1 = \bar{y}_0 - \epsilon \left(\mathcal{Y}_{x_*}^1(1) + \left(\frac{1}{x_f} - 1\right) \ln\left(\frac{x_* - x_f}{1 - x_f}\right) \right) = \bar{y}_0 - \epsilon \int_{x_*}^1 \left(\frac{x_*}{u} - 1\right) \left(\frac{1}{u} - 1\right) \frac{1}{Y_0^{\text{out}}(u)} du. \quad (24)$$

148 In Appendix A.2, we derive a closed-form analytical approximation to the integral in Equation (24), which
 149 then yields

$$149 \quad \bar{y}_1 \approx 1 - x_*(1 - \ln x_*) - \epsilon \frac{(1 - x_*)(1 - x_* + \ln x_*)}{1 - x_*(1 - \ln x_*)}. \quad (25)$$

150 3.3 Outer to corner solution matching

151 We start by introducing an intermediate scale $\eta = \eta(\epsilon)$ that we will use to capture the overlap between the
 152 outer and corner solutions:

$$153 \quad \epsilon \ln \epsilon^{-1} \ll \eta \ll \epsilon^{1/2}, \quad (26)$$

which implies

$$154 \quad \eta^2 \ll \epsilon \ll \epsilon \ln \eta^{-1} \ll \epsilon \ln \epsilon^{-1} \ll \eta. \quad (27)$$

154 In addition, $\epsilon \ln \epsilon^{-1} \ll \eta$ implies that $\frac{1}{\epsilon} e^{-\frac{\eta x_\eta}{\epsilon}} C \ll 1$ for any $C > 0$. Expanding the outer solution $Y(x; \epsilon)$ (21)
 155 about $x = x_f + \eta x_\eta$ in an asymptotic series with these orders gives us

$$156 \quad Y^{\text{out}}(x_f + \eta x_\eta; \epsilon) = \eta \left(\frac{x_*}{x_f} - 1 \right) x_\eta - \epsilon \ln \eta^{-1} \left(\frac{1}{x_f} - 1 \right) \\ 157 \quad + \epsilon \left(\left(\frac{1}{x_f} - 1\right) \ln x_\eta - \left(\frac{1}{x_f} - 1\right) \ln(1 - x_f) - \mathcal{Y}_{x_f}^1(1) \right) + \mathcal{O}(\eta^2). \quad (28)$$

159 To match Y^{out} with the corner layer solution $X^{\text{cor}}(y; \epsilon)$ [Table 1], we must first re-express it as a function
 160 $Y^{\text{cor},i}(x; \epsilon)$ of x . Rearranging $x = X^{\text{cor}}(y; \epsilon)$, we get

$$161 \quad -\frac{1}{\epsilon} \left(\frac{1}{\frac{\text{cor}}{C_0}} - 1 \right)^{-1} e^{-\frac{1}{\epsilon} \frac{x_* - \frac{\text{cor}}{C_0}}{1 - \frac{\text{cor}}{C_0}}} \left(x - \frac{\text{cor}}{C_0} - \epsilon \ln \epsilon^{-1} \left(C \ln + \frac{1 - \frac{\text{cor}}{C_0}}{x_* - \frac{\text{cor}}{C_0}} \right) - \epsilon C_1 \right) = -\frac{1}{\epsilon} \left(\frac{1}{\frac{\text{cor}}{C_0}} - 1 \right)^{-1} y e^{-\frac{1}{\epsilon} \left(\frac{1}{\frac{\text{cor}}{C_0}} - 1 \right)^{-1} y} \quad (29)$$

162

$$= \mathcal{E} \left(-\frac{1}{\epsilon} \left(\frac{1}{C_0^{\text{cor}}} - 1 \right)^{-1} y \right), \quad (30)$$

163 which we can invert using the Lambert W function to get $y = Y^i(x; \epsilon)$:

$$Y^i(x; \epsilon) = -\epsilon \left(\frac{1}{C_0^{\text{cor}}} - 1 \right) W_i \left(-\frac{1}{\epsilon} \left(\frac{1}{C_0^{\text{cor}}} - 1 \right)^{-1} e^{-\frac{1}{\epsilon} \frac{x_* - C_0^{\text{cor}}}{1 - C_0^{\text{cor}}} \left(x - C_0^{\text{cor}} - \epsilon \ln \epsilon^{-1} \left(C_{\text{ln}}^{\text{cor}} + \frac{1 - C_0^{\text{cor}}}{x_* - C_0^{\text{cor}}} \right) - \epsilon C_1^{\text{cor}} \right)} \right), \quad (31)$$

164 where $i = -1, 0$ correspond to values of $y \geq \epsilon \left((1/C_0^{\text{cor}}) - 1 \right)$ and $y \leq \epsilon \left((1/C_0^{\text{cor}}) - 1 \right)$, respectively. Note that the
 165 point $\left(C_0^{\text{cor}}, \epsilon \left((1/C_0^{\text{cor}}) - 1 \right) \right)$ is on the x nullcline, $\frac{dX}{d\tau} = 0$, *i.e.*, $y = \epsilon \left(\frac{1}{x} - 1 \right)$, which separates the upper and
 166 lower branches of the phase-plane trajectories. The two branches $i = -1, 0$ give the solutions above and below
 167 the nullcline, which we match to the outer solution $Y^{\text{out}}(x; \epsilon)$ (21) and the x -axis boundary layer solution,
 168 $Y^{\text{xb}}(x; \epsilon)$ [Table 1], respectively.

169 If we set $x = C_0^{\text{cor}} + \eta x_\eta$ in Equation (31), and note that by Equation (26),

$$1 \ll \ln \epsilon^{-1} \ll \frac{\eta}{\epsilon}, \quad (32)$$

170 we can infer that the argument of the Lambert W function in Equation (31) is proportional to

$$e^{-\frac{\eta}{\epsilon} \frac{x_* - C_0^{\text{cor}}}{1 - C_0^{\text{cor}}} x_\eta - \ln \epsilon^{-1}} \sim e^{-\frac{\eta}{\epsilon} \frac{x_* - C_0^{\text{cor}}}{1 - C_0^{\text{cor}}} x_\eta}. \quad (33)$$

171 If $C_0^{\text{cor}} < x_*$ and $x_\eta > 0$, the argument vanishes as $\eta \rightarrow 0$ and we can use the expansion of W_{-1} for small
 172 arguments [3],

$$W_{-1}(z) = \ln(-z) - \ln(-\ln(-z)) + o(1), \quad (34)$$

173 to expand $Y^{\text{cor}-1}(x; \epsilon)$ about $x_\eta = 0$ and obtain

$$\begin{aligned} Y^{\text{cor}-1}(C_0^{\text{cor}} + \eta x_\eta; \epsilon) &= \eta \left(\frac{x_*}{C_0^{\text{cor}}} - 1 \right) x_\eta - \epsilon \ln \eta^{-1} \left(\frac{1}{C_0^{\text{cor}}} - 1 \right) - \epsilon \ln \epsilon^{-1} \left(\frac{x_*}{C_0^{\text{cor}}} - 1 \right) \left(C_{\text{ln}}^{\text{cor}} + \frac{1 - C_0^{\text{cor}}}{x_* - C_0^{\text{cor}}} \right) \\ &+ \epsilon \left[\left(\frac{1}{C_0^{\text{cor}}} - 1 \right) \ln x_\eta + \left(\frac{1}{C_0^{\text{cor}}} - 1 \right) \ln \left(\frac{x_*}{C_0^{\text{cor}}} - 1 \right) - \left(\frac{x_*}{C_0^{\text{cor}}} - 1 \right) C_1^{\text{cor}} \right] + \mathcal{O} \left(\frac{\epsilon^2 \ln \epsilon^{-1}}{\eta} \right). \end{aligned} \quad (35)$$

177 Note that $\epsilon \ln \epsilon^{-1} \ll \eta$ implies $\frac{\epsilon^2 \ln \epsilon^{-1}}{\eta} \ll \epsilon$ and the two solutions, $Y^{\text{out}}(x_f + \eta x_\eta; \epsilon)$ and $Y^{\text{cor}-1}(x_f + \eta x_\eta; \epsilon)$, agree
 178 up to $\mathcal{O}(\epsilon)$ provided we set

$$C_0^{\text{cor}} = x_f, \quad (36)$$

$$C_{\text{ln}}^{\text{cor}} = -\frac{1 - C_0^{\text{cor}}}{x_* - C_0^{\text{cor}}} = -\frac{1 - x_f}{x_* - x_f}, \quad (37)$$

181 and

$$C_1^{\text{cor}} = \frac{1 - x_f}{x_* - x_f} \left[\ln \left(\left(\frac{1}{x_f} - 1 \right) (x_* - x_f) \right) + \left(\frac{1}{x_f} - 1 \right)^{-1} \mathcal{Y}_{x_f}^1(1) \right]. \quad (38)$$

183 Substituting these choices into Equation (31) yields a matched **left corner solution** at x_f ,

$$184 \quad Y^{\text{lc}}(x; \epsilon) = -\epsilon \left(\frac{1}{x_f} - 1 \right) W_i \left(-\frac{x_* - x_f}{\epsilon} e^{-\frac{x-x_f}{\epsilon} \frac{x_* - x_f}{1-x_f} + \left(\frac{1}{x_f} - 1 \right)^{-1} \mathcal{Y}_{x_f}^1(1)} \right). \quad (39)$$

185 Summing the $i = -1$ branch, $Y^{-1}(x; \epsilon)$, and the outer solution, $Y^{\text{out}}(x; \epsilon)$, and then subtracting the overlap,
186 yields a matched solution for the region above the x nullcline,

$$187 \quad Y^\dagger(x; \epsilon) = Y_0^{\text{out}}(x) + Y^{-1}(x; \epsilon) - \left(\frac{x_*}{x_f} - 1 \right) (x - x_f) + \epsilon \mathcal{Y}_{x_f}^x(1). \quad (40)$$

188 **Applicability of the first order solution** Some care is required in applying the results above; $|\mathcal{Y}_{x_f}^x(1)|$
189 grows very rapidly with increasing \mathcal{R}_0 , so $\epsilon |\mathcal{Y}_{x_f}^x(1)|$ need not be small (*e.g.*, $\epsilon |\mathcal{Y}_{x_f}^x(1)| \approx 4.4$ for $\mathcal{R}_0 = 6$ and
190 $\epsilon = 0.01$), so there are realistic parameter regimes where higher order terms would be necessary to obtain a
191 good approximation. In Appendix B we derive upper bounds on the admissible values of ϵ as a function of
192 \mathcal{R}_0 .

193 3.4 Corner to Inner Solution Matching

194 We can similarly match the $i = 0$ branch, $Y^0(x; \epsilon)$, to the x -axis boundary layer solution $Y^{\text{xb}}(x; \epsilon)$ [Table 1],
195 As we observed in the previous subsection, if we set $x = x_f + \eta x_\eta$, the argument of the W function in
196 $Y^0(x_f + \eta x_\eta; \epsilon)$ is small [see Equation (39)]. Because we are now using the $i = 0$ branch instead of $i = -1$, we
197 use the expansion $W_0(z) = z + \mathcal{O}(z^2)$ [3] to get

$$198 \quad Y^0(x_f + \eta x_\eta; \epsilon) = \left(\frac{1}{x_f} - 1 \right) (x_* - x_f) e^{-\frac{\eta x_\eta}{\epsilon} \frac{x_* - x_f}{1-x_f} + \left(\frac{1}{x_f} - 1 \right)^{-1} \mathcal{Y}_{x_f}^1(1)} + \mathcal{O} \left(e^{-2\frac{\eta x_\eta}{\epsilon} \frac{x_* - x_f}{1-x_f}} \right). \quad (41)$$

199 On the other hand, substituting $C_0^\phi = c_0^\phi - (1 - x_*) \ln(1 - c_0^\phi)$ into the x -axis boundary layer solution
200 [Table 1] gives

$$Y^{\text{xb}}(x; \epsilon) = \left(\frac{1-x}{1-c_0^\phi} \right)^{-\frac{1}{\epsilon}(1-x_*)} e^{\frac{1}{\epsilon}(c_0^\phi - x) + C_1^\phi}. \quad (42)$$

201 Evaluating at $x = c_0^\phi + \eta x_\eta$, we have

$$\begin{aligned} 202 \quad Y^{\text{xb}}(c_0^\phi + \eta x_\eta; \epsilon) &= \left(1 - \frac{\eta x_\eta}{1 - c_0^\phi} \right)^{-\frac{1-x_*}{\epsilon}} e^{-\frac{\eta x_\eta}{\epsilon} + C_1^\phi} \\ &= e^{-\frac{\eta x_\eta}{\epsilon} - \frac{1-x_*}{\epsilon} \ln \left(1 - \frac{\eta x_\eta}{1 - c_0^\phi} \right) + C_1^\phi} \\ 203 \quad &= e^{-\frac{\eta x_\eta}{\epsilon} \frac{x_* - c_0^\phi}{1 - c_0^\phi} + C_1^\phi + \mathcal{O} \left(\frac{\eta^2}{\epsilon} \right)} \\ 204 \quad &= e^{-\frac{\eta x_\eta}{\epsilon} \frac{x_* - c_0^\phi}{1 - c_0^\phi} + C_1^\phi} \left(1 + \mathcal{O} \left(\frac{\eta^2}{\epsilon} \right) \right), \end{aligned} \quad (43)$$

205 and the solutions (41, 43) coincide if we take

$$207 \quad c_0^\phi = x_f \quad (44)$$

$$208 \quad C_0^\phi = c_0^\phi - (1 - x_*) \ln(1 - c_0^\phi) = x_f - (1 - x_*) \ln(1 - x_f) \quad (45)$$

209 and

$$210 \quad C_1^\phi = \ln \left[\left(\frac{1}{x_f} - 1 \right) (x_* - x_f) \right] + \left(\frac{1}{x_f} - 1 \right)^{-1} \mathcal{Y}_{x_f}^1(1). \quad (46)$$

211 Substituting these choices into $\overset{xb}{Y}(x; \epsilon)$ [Table 1] gives

$$212 \quad \overset{xb}{Y}(x; \epsilon) = \left(\frac{1}{x_f} - 1 \right) (x_* - x_f) \left(\frac{1 - x_f}{1 - x} \right)^{\frac{1 - x_*}{\epsilon}} e^{-\frac{x - x_f}{\epsilon} + \left(\frac{1}{x_f} - 1 \right)^{-1}} \mathcal{Y}_{x_f}^1(1). \quad (47)$$

213 As we observed in [10], we can write $\overset{xb}{Y}(x; \epsilon) = (1/x_f - 1)(x_* - x_f) e^{\left(\frac{1}{x_f} - 1 \right)^{-1}} \mathcal{Y}_{x_f}^1(1) e^{-\frac{\phi_0(x)}{\epsilon}}$, for

$$\phi_0(x) = x - x_f + (1 - x_*) \ln \left(\frac{1 - x}{1 - x_f} \right). \quad (48)$$

214 $\phi_0(x)$ has two zeros, at x_f and $x_{i,2}$ [Equations (9) and (12)]. Between these two zeros, $\phi_0(x) > 0$ and—
 215 excluding small neighbourhoods [of radius $\mathcal{O}(\epsilon \ln \epsilon^{-1})$] of the two zeroes— $\overset{xb}{Y}(x; \epsilon)$ will be transcendently
 216 small in the interval $(x_f, x_{i,2})$. The small neighbourhoods of the zeros of $\phi_0(x)$, where $\overset{xb}{Y}(x; \epsilon) = \mathcal{O}(\epsilon)$, provide
 217 a “transition-zone” where we can match the boundary layer solution with the corner solutions (also $\mathcal{O}(\epsilon)$)
 218 and via them, with the outer solution (which is $\mathcal{O}(1)$).

219 Expanding in series exactly as we did above with the left corner solution $\overset{lc}{Y}^0(x; \epsilon)$ (39), we match $\overset{xb}{Y}(x; \epsilon)$
 220 (47) to $\overset{cor}{Y}^i(x; \epsilon)$ (31) to get a **right corner solution** at $x_{i,2}$:

$$221 \quad \overset{rc}{Y}^i(x; \epsilon) = -\epsilon \left(\frac{1}{x_{i,2}} - 1 \right) W_i \left(-\frac{\left(\frac{1}{x_f} - 1 \right) (x_* - x_f)}{\epsilon \left(\frac{1}{x_{i,2}} - 1 \right)} e^{-\frac{x_{i,2} - x}{\epsilon} \frac{x_{i,2} - x_*}{1 - x_{i,2}} + \left(\frac{1}{x_f} - 1 \right)^{-1}} \mathcal{Y}_{x_f}^1(1) \right) \quad (49)$$

(for the sake of completeness, we list the matching constants in Table 4).

222 Summing the two corner solutions [Equations (39) and (49), taking the $i = 0$ branches for the solutions
 223 below the x nullcline] and the x -axis boundary layer solution (47), and subtracting the resulting overlaps,
 224 yields a matched solution below the x nullcline,

$$225 \quad Y_\downarrow(x; \epsilon) = \overset{xb}{Y}(x; \epsilon) + \overset{lc}{Y}^0(x; \epsilon) + \overset{rc}{Y}^0(x; \epsilon) - \left(\frac{1}{x_f} - 1 \right) (x_* - x_f) e^{\left(\frac{1}{x_f} - 1 \right)^{-1}} \mathcal{Y}_{x_f}^1(1) \left(e^{-\frac{x - x_f}{\epsilon} \frac{x_* - x_f}{1 - x_f}} + e^{-\frac{x_{i,2} - x}{\epsilon} \frac{x_{i,2} - x_*}{1 - x_{i,2}}} \right). \quad (50)$$

225 3.4.1 Prevalence trough

226 Evaluating $\overset{xb}{Y}(x; \epsilon)$ (47) at $x = x_*$ gives us an estimate of the minimum fraction infected (\underline{y}),

$$227 \quad \underline{y}_1 = \left(\frac{1}{x_f} - 1 \right) (x_* - x_f) \left(\frac{1 - x_f}{1 - x_*} \right)^{\frac{1 - x_*}{\epsilon}} e^{-\frac{x_* - x_f}{\epsilon} + \left(\frac{1}{x_f} - 1 \right)^{-1}} \mathcal{Y}_{x_f}^1(1). \quad (51)$$

228 Figure 3 shows the accuracy of this approximation to \underline{y} .

229 3.4.2 Closed-form approximations

230 Using our approximation to $\mathcal{Y}_{x_f}^1(1)$ [Equation (A.1.1) in Appendix A], we obtain

$$\left(\frac{1}{x_f} - 1 \right)^{-1} \mathcal{Y}_{x_f}^1(1) \approx \frac{x_* - x_f + x_* x_f}{(1 - x_f)(1 - x_*)} \ln x_f - \frac{x_*}{x_* - x_f}. \quad (52)$$

231 Substituting Equation (52) into Equations (39), (47) and (49) to (51) gives us closed-form analytical expres-
 232 sions for all but the outer solution, $\overset{\text{out}}{Y}(x; \epsilon)$, which depends on $\mathcal{Y}_x^1(1)$ (we do not have a good approximation
 233 for the integral $\mathcal{Y}_x^1(1)$ for arbitrary x). We present these closed-form solutions in Tables 2 and 3.

234 3.5 Beyond the first epidemic wave

235 In principle, we could continue our phase plane trajectory approximation through any number of epidemic
 236 waves, but unlike the simple iterative expression we obtained in [10], the higher order expressions rapidly
 237 increase in complexity, and we have not identified a pattern that allows us to simplify them.

238 To illustrate the growth in analytical complexity as the trajectory proceeds, we will briefly sketch the
 239 derivation of the solution $Y^\dagger(x; \epsilon)$ for the *second* epidemic wave. The $i = -1$ branch of the right corner
 240 solution (49) extends the solution above the x nullcline.

241 To match into the outer solution $\overset{\text{out}}{Y}(x, x_{i,2}; \epsilon)$ [Equations (20) and (21)], we expand $\overset{\text{rc}}{Y}^{-1}(x; \epsilon)$ as usual
 242 in an asymptotic series. Since the trajectory always lies in the set $x < x_{i,2}$, we make the change of variables
 243 $x = x_{i,2} - \eta x_\eta$ in $\overset{\text{rc}}{Y}^{-1}(x; \epsilon)$ and expand using Equation (34) to get

$$\begin{aligned}
 \overset{\text{rc}}{Y}^{-1}(x_{i,2} - \eta x_\eta; \epsilon) &= -\epsilon \left(\frac{1}{x_{i,2}} - 1 \right) W_{-1} \left(-\frac{1}{\epsilon} \frac{\left(\frac{1}{x_f} - 1 \right) (x_* - x_f) e^{-\frac{\eta x_\eta}{\epsilon} \frac{x_{i,2} - x_*}{1 - x_{i,2}}} - \left(\frac{1}{x_f} - 1 \right)^{-1} \mathcal{Y}_{x_f}^1(1)}{\left(\frac{1}{x_{i,2}} - 1 \right)} \right) \\
 &= \eta \left(1 - \frac{x_*}{x_{i,2}} \right) x_\eta + \epsilon \ln \eta^{-1} \left(\frac{1}{x_{i,2}} - 1 \right) \\
 &\quad - \epsilon \left(\frac{1}{x_{i,2}} - 1 \right) \left[\ln x_\eta + \ln \left(\frac{\left(\frac{1}{x_f} - 1 \right) (x_* - x_f) (1 - x_{i,2})}{\left(\frac{1}{x_{i,2}} - 1 \right) (x_{i,2} - x_*)} \right) - \left(\frac{1}{x_f} - 1 \right)^{-1} \mathcal{Y}_{x_f}^1(1) \right] \\
 &\quad + \mathcal{O} \left(\frac{\epsilon^2 \ln \epsilon^{-1}}{\eta} \right), \tag{53}
 \end{aligned}$$

248 which has a logarithmic singularity at $x_{i,2}$. While this singularity may initially appear to be a defect in
 249 the approximation, it is necessary to match to the outer solution for the second epidemic wave (21): once
 250 we impose the effective initial condition $x_{i,2} < 1$ (12), the second wave outer solution also has a logarithmic
 251 singularity at $x_{i,2}$.

252 Expanding $\overset{\text{out}}{Y}(x, x_{i,2}; \epsilon)$ [Equations (20) and (21)] about $x = x_{i,2}$, we have

$$\begin{aligned}
 \overset{\text{out}}{Y}(x_{i,2} - \eta x_\eta, x_{i,2}; \epsilon) &= \eta \left(1 - \frac{x_*}{x_{i,2}} \right) x_\eta - \epsilon \ln \eta^{-1} \left(\frac{1}{x_{i,2}} - 1 \right) \\
 &\quad + \epsilon \left(\left(\frac{1}{x_{i,2}} - 1 \right) \ln x_\eta + \mathcal{Y}_{x_*}^{x_{i,2}}(x_{i,2}) - \left(\frac{1}{x_{i,2}} - 1 \right) \ln(x_{i,2} - x_*) + \left(\frac{1}{x_{f,2}} - 1 \right) \ln \left(\frac{x_{i,2} - x_{f,2}}{x_* - x_{f,2}} \right) + C_1^{\text{out}} \right) \\
 &\quad + \mathcal{O}(\eta^2), \tag{54}
 \end{aligned}$$

256 where

$$x_{f,2} = x_f(x_{i,2}) \tag{55}$$

257 is the “final size” of the second epidemic wave.

258 Note that the offending logarithmic term from Equation (53) appears with opposite sign in Equation (54):
 259 when we sum the two solutions, the singularities will cancel. Choosing

$$C_1^{\text{out}} = - \left(\frac{1}{x_{f,2}} - 1 \right) \ln \left(\frac{x_{i,2} - x_{f,2}}{x_* - x_{f,2}} \right) - \left(\frac{1}{x_{i,2}} - 1 \right) \ln \left(\frac{\left(\frac{1}{x_f} - 1 \right) (x_* - x_f) (1 - x_{i,2})}{\left(\frac{1}{x_{i,2}} - 1 \right)} \right) + \frac{\frac{1}{x_{i,2}} - 1}{\frac{1}{x_f} - 1} \mathcal{Y}_{x_f}^1(1) - \mathcal{Y}_{x_*}^{x_{i,2}}(x_{i,2}) \tag{56}$$

260 so that the expansions (53) and (54) agree to $\mathcal{O}(\epsilon)$ one obtains

$$\begin{aligned} Y_0^{\text{out}}(x, x_{i,2}) + \epsilon \left[-\mathcal{Y}_{x_{i,2}}^{x_{i,2}}(x_{i,2}) + \left(\frac{1}{x_{i,2}} - 1 \right) \ln \left(\frac{x_{i,2} - x}{1 - x_{i,2}} \right) + \left(\frac{1}{x_{f,2}} - 1 \right) \ln \left(\frac{x - x_{f,2}}{x_{i,2} - x_{f,2}} \right) \right. \\ \left. + \frac{\frac{1}{x_{i,2}} - 1}{\frac{1}{x_f} - 1} \mathcal{Y}_{x_f}^1(1) - \left(\frac{1}{x_{i,2}} - 1 \right) \ln \left(\frac{\left(\frac{1}{x_f} - 1 \right) (x_* - x_f)}{\left(\frac{1}{x_{i,2}} - 1 \right) (x_{i,2} - x_*)} \right) \right] \end{aligned} \quad (57)$$

261 Finally, replacing x_f by $x_{f,2}$ in the left corner solution (39) and its expansion (35) gives us the second
 262 left-corner solution and its expansion (up to the unknown matching constant $\overset{\text{cor}}{C}_1$). Comparing (35) (suitably
 263 modified with $x_{f,2}$ replacing x_f) with (54) (for the appropriate choice of $\overset{\text{out}}{C}_1$), we again determine $\overset{\text{cor}}{C}_1$ by
 264 requiring the series agree to $\mathcal{O}(\epsilon)$. This yields

$$\begin{aligned} Y^{\text{lc}}(x; \epsilon) = -\epsilon \left(\frac{1}{x_{f,2}} - 1 \right) W_i \left(-\frac{x_{i,2} - x_{f,2}}{\epsilon} \left(\frac{x_* - x_{f,2}}{1 - x_{f,2}} \right) \left(\frac{\left(\frac{1}{x_f} - 1 \right) (x_* - x_f) (1 - x_{i,2})}{\left(\frac{1}{x_{i,2}} - 1 \right) (x_{i,2} - x_*) (x_{i,2} - x_{f,2})} \right)^{\frac{\frac{1}{x_{i,2}} - 1}{\frac{1}{x_{f,2}} - 1}} \right) \\ \times \exp \left(-\frac{x - x_{f,2}}{\epsilon} \frac{x_* - x_{f,2}}{1 - x_{f,2}} + \left(\frac{1}{x_{f,2}} - 1 \right)^{-1} \mathcal{Y}_{x_{f,2}}^{x_{i,2}}(x_{i,2}) + \frac{\left(\frac{1}{x_{i,2}} - 1 \right)}{\left(\frac{1}{x_f} - 1 \right) \left(\frac{1}{x_{f,2}} - 1 \right)} \mathcal{Y}_{x_f}^1(1) \right), \end{aligned} \quad (58)$$

266 whereas the matched solution above the x nullcline is

$$\begin{aligned} Y_0^{\text{out}}(x, x_{i,2}) + Y^{\text{rc}}(x; \epsilon) + Y^{\text{lc}}(x; \epsilon) - \left(1 - \frac{x_*}{x_{i,2}} \right) (x_{i,2} - x) - \left(\frac{x_*}{x_{f,2}} - 1 \right) (x - x_{f,2}) \\ + \epsilon \left[\mathcal{Y}_{x_{f,2}}^x(x_{i,2}) + \frac{\left(\frac{1}{x_{i,2}} - 1 \right)}{\left(\frac{1}{x_f} - 1 \right)} \mathcal{Y}_{x_f}^1(1) + \left(\frac{1}{x_{i,2}} - 1 \right) \ln \left(\frac{\left(\frac{1}{x_f} - 1 \right) (x_* - x_f) (1 - x_{i,2})}{\left(\frac{1}{x_{i,2}} - 1 \right) (x_{i,2} - x_*) (x_{i,2} - x_{f,2})} \right) \right] \end{aligned} \quad (59)$$

268 While one might hope to recognize a pattern that facilitates continuing the approximation through subsequent
 269 waves, we have not succeeded and do not pursue the question further. We leave it as an exercise for the
 270 motivated reader.

271 4 Discussion

272 Building on our previous work [10], we have developed a higher order approximation for the phase plane
 273 trajectories of the standard SIR model with vital dynamics Equation (4). Throughout the phase plane, the
 274 “first order” solution we have presented here is more accurate than the “zeroth order” solution we derived
 275 previously [10], but the higher order results are much more cumbersome and, in practice, useful only until
 276 the peak of the second epidemic wave (whereas our “zeroth order” approximation is useful for an arbitrary
 277 number of epidemic waves). Much of the “first order” gain in accuracy is in the part of the phase plane
 278 where the frequency of infected hosts is implausibly low (reminiscent of Mollison’s “atto-fox” [7]).

279 Our higher order trajectory approximation (Y^\dagger and Y_\dagger in Table 3) depends on an integral that must be
 280 evaluated numerically [$\mathcal{Y}_a^b(x_i)$, Equation (18)]. However, as noted in §3.4.2, our closed-form approximation
 281 (52) to $\mathcal{Y}_{x_f}^1(1)$ allows us to obtain closed-form analytical expressions for all components of our matched
 282 asymptotic expansion *except* the outer solution. Our most useful closed-form results are our expressions for

283 the maximum and minimum prevalence following disease invasion (\bar{y} in Equation (25) and \underline{y} in Equation (51)
284 using Equation (52)). We emphasize that our peak prevalence formula (25) includes the first order effect of
285 demography, whereas in [10] our peak prevalence formula was the same as KM's.

286 Acknowledgements

287 This project was partially supported by the CNRS IEA grant "Structured Populations, Epidemics & Control
288 Strategies (SPECS)". DJDE was supported by an NSERC Discovery Grant.

289 References

- 290 [1] C. M. Bender and S. A. Orszag. *Advanced Mathematical Methods for Scientists and Engineers*. McGraw-
291 Hill, New York, 1978.
- 292 [2] G. Birkhoff, M. H. Schultz, and R. S. Varga. Piecewise Hermite interpolation in one and two variables
293 with applications to partial differential equations. *Numer. Math.*, 11(3):232–256, 1968.
- 294 [3] R. M. Corless, G. H. Gonnet, D. E. G. Hare, D. J. Jeffrey, and D. E. Knuth. On the Lambert W
295 function. *Adv. Comput. Math.*, 5(1):329–359, Dec 1996.
- 296 [4] J. F. Epperson. On the Runge example. *Am. Math. Mon.*, 94(4):329–341, 1987.
- 297 [5] W. O. Kermack and A. G. McKendrick. A contribution to the mathematical theory of epidemics. *Proc.*
298 *R. Soc. A*, 115:700–721, 1927.
- 299 [6] J. Kevorkian and J. D. Cole. *Multiple Scale and Singular Perturbation Methods*. Springer-Verlag New
300 York Inc., New York, 1996.
- 301 [7] D. Mollison. Dependence of epidemic and population velocities on basic parameters. *Math. Biosci.*,
302 107:255–287, 1991.
- 303 [8] R. E. O'Malley, Jr. *Singular Perturbation Methods for Ordinary Differential Equations*, volume 89.
304 Springer, 1991.
- 305 [9] T. L. Parsons, B. M. Bolker, J. Dushoff, and D. J. D. Earn. The probability of epidemic burnout in the
306 stochastic SIR model with demography. in preparation, 2023.
- 307 [10] Todd L. Parsons and David J. D. Earn. Analytical approximations for the phase plane trajectories of
308 the SIR model with vital dynamics. preprint, <https://cnrs.hal.science/hal-04178969>.
- 309 [11] O. A. van Herwaarden. Stochastic epidemics: the probability of extinction of an infectious disease at
310 the end of a major outbreak. *J. Math. Biol.*, 35(7):793–813, 1997.

311 A Analytical Approximations for $\mathcal{Y}_a^b(x_i)$

312 A.1 Approximating $\mathcal{Y}_{x_f(x_i)}^{x_i}(x_i)$

313 While simple to formulate, in addition to having no analytical closed form, the integral (18) proves in-
 314 convenient to compute numerically. Here we consider analytical approximations obtained via polynomial
 315 approximations to $Y_0^{\text{out}}(x, x_i)$. In order to be consistent with our matchings, we require that the approxima-
 316 tion preserve the poles and residues of the integrand, or equivalently that we approximate $Y_0^{\text{out}}(x, x_i)$ by a
 317 polynomial with the same zeros x_i and x_f , and the same derivatives at these points, $\frac{x_*}{x_i} - 1$ and $\frac{x_*}{x_f} - 1$.

318 When $x_i = 1$, the singularity at x_i is removable, and we can approximate $Y_0^{\text{out}}(x) = Y_0^{\text{out}}(x, 1)$ by its linear
 319 approximation at x_f , $L(x, 1) = \left(\frac{x_*}{x_f} - 1\right)(x - x_f)$. This gives us a particularly simple analytical expression,

$$\begin{aligned} \mathcal{Y}_x^1(1) &= \int_x^1 \left[\left(\frac{x_*}{u} - 1\right) \left(\frac{1}{u} - 1\right) \frac{1}{Y_0^{\text{out}}(u)} - \left(\frac{1}{x_f} - 1\right) \frac{1}{u - x_f} \right] du \\ &\approx \int_x^1 \left[\left(\frac{x_*}{u} - 1\right) \left(\frac{1}{u} - 1\right) \frac{1}{L(u, 1)} - \left(\frac{1}{x_f} - 1\right) \frac{1}{u - x_f} \right] du \\ &= \left(\frac{1}{x_f} - 1 - \frac{x_f}{x_* - x_f}\right) \ln x - \frac{x_*}{x_* - x_f} \left(\frac{1}{x} - 1\right). \end{aligned} \quad (\text{A.1.1})$$

320 For $x = x_f$, the value of the integral is largely determined in a neighbourhood of x_f and Equation (A.1.1)
 321 agrees very well with the numerically computed value of $\mathcal{Y}_{x_f}^1(1)$ (Figure 1). Unfortunately, Equation (A.1.1)
 322 fails to provide a good uniform approximation for generic x .

323 For a general initial condition x_i , we can approximate $Y_0^{\text{out}}(x, x_i)$ by the cubic Hermite spline [2] determined
 324 by its zeroes and the derivatives at the zeroes:

$$\begin{aligned} H(x, x_i) &= \left(\frac{x_*}{x_i} - 1\right)(x - x_i) + \frac{\frac{x_*}{x_i} - 1}{x_i - x_f(x_i)}(x - x_i)^2 + \frac{\left(\frac{x_*}{x_i} - 1\right) + \left(\frac{x_*}{x_f(x_i)} - 1\right)}{(x_i - x_f(x_i))^2}(x - x_i)^2(x - x_f(x_i)) \\ &= \frac{\left(\frac{x_*}{x_i} - 1\right) + \left(\frac{x_*}{x_f(x_i)} - 1\right)}{(x_i - x_f(x_i))^2}(x - x_i)(x - x_f(x_i))(x - x_H(x_i)) \end{aligned} \quad (\text{A.1.2})$$

325 where

$$x_H(x_i) = \frac{\left(\frac{x_*}{x_i} - 1\right)x_f(x_i) + \left(\frac{x_*}{x_f(x_i)} - 1\right)x_i}{\left(\frac{x_*}{x_i} - 1\right) + \left(\frac{x_*}{x_f(x_i)} - 1\right)} \quad (\text{A.1.3})$$

326 is the third root of the Hermite spline $H(x, x_i)$.

327 We then have

$$\begin{aligned} \mathcal{Y}_x^{x_i}(x_i) &= \int_x^{x_i} \left[\left(\frac{1}{u} - 1\right) \left(\frac{x_*}{u} - 1\right) \frac{1}{Y_0^{\text{out}}(u, x_i)} - \left(\frac{1}{x_i} - 1\right) \frac{1}{u - x_i} - \left(\frac{1}{x_f(x_i)} - 1\right) \frac{1}{u - x_f(x_i)} \right] du \\ &\approx \int_x^{x_i} \left[\left(\frac{1}{u} - 1\right) \left(\frac{x_*}{u} - 1\right) \frac{1}{H(u, x_i)} - \left(\frac{1}{x_i} - 1\right) \frac{1}{u - x_i} - \left(\frac{1}{x_f(x_i)} - 1\right) \frac{1}{u - x_f(x_i)} \right] du \\ &= -\frac{(x_i - x_f(x_i))^2}{\left(\frac{x_*}{x_i} - 1\right) + \left(\frac{x_*}{x_f(x_i)} - 1\right)} \left[\frac{x_*}{x_i x_f(x_i) x_H(x_i)} \left(\frac{1}{x} - \frac{1}{x_i} + \left(1 + \frac{1}{x_*} - \frac{1}{x_i} - \frac{1}{x_f(x_i)} - \frac{1}{x_H(x_i)}\right) \ln\left(\frac{x}{x_i}\right)\right) \right. \\ &\quad \left. + \frac{\left(\frac{x_*}{x_H(x_i)} - 1\right) \left(\frac{1}{x_H(x_i)} - 1\right)}{(x_H(x_i) - x_i)(x_H(x_i) - x_f(x_i))} \ln\left(\frac{x - x_H(x_i)}{x_i - x_H(x_i)}\right) \right]. \end{aligned} \quad (\text{A.1.4})$$

Equation (A.1.4) provides a good approximation that is uniform in x , *provided* \mathcal{R}_0 is close to 1. Away from this limit, Equation (A.1.4) performs similarly to Equation (A.1.1), *i.e.*, it does not provide a good uniform approximation in x , but for $x = x_f(x_i)$ (for a general x_i) it does approximate $\mathcal{Y}_{x_f(x_i)}^{x_i}(x_i)$ very well (*cf.* Equations (58) and (59) and Figure 1). The failure for general \mathcal{R}_0 is due to the Hermite cubic spline substantially overestimating \bar{y} for larger values of \mathcal{R}_0 , which results in a poor approximation to $\mathcal{Y}_{x_i}^{x_i}(x_i)$ for x near to x_* . We attempted to obtain an improved estimate to $\bar{Y}_0^{\text{out}}(x, x_i)$ by imposing a maximum at $(x_*, \bar{y}_0(x_i))$, either by using a pair of cubic Hermite splines on the intervals $[x_f(x_i), x_*]$ and $[x_*, x_i]$ or by using a quintic Hermite spline; unfortunately, the resulting approximations are overwhelmed by Runge oscillations [4].

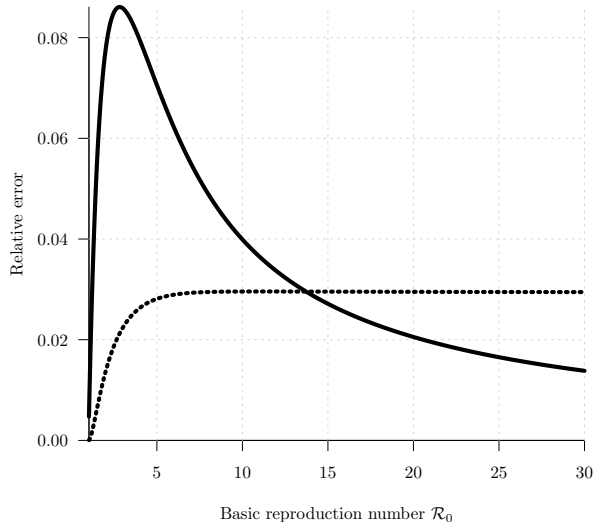


Figure 1: Relative error in our numerical approximations of $\mathcal{Y}_{x_{f,j}}^{x_{i,j}}(x_{i,j})$ for $j = 1$ (solid) and $j = 2$ (dotted). The exact expression as an integral is given in Equation (18). The closed-form approximations are given in Equations (A.1.1) and (A.1.4).

337 A.2 Approximating \bar{y}

338 We can obtain an excellent explicit approximation to

$$\mathcal{Y}_{\text{max}} = \int_{x_*}^1 \left(\frac{x_*}{u} - 1 \right) \left(\frac{1}{u} - 1 \right) \frac{1}{Y_0^{\text{out}}(u)} du \quad (\text{A.2.1})$$

339 (see Equation (24)) by approximating $\bar{Y}_0^{\text{out}}(u)$ with a rational function on the interval $[x, 1]$. The simplest
 340 rational approximation is the line joining $(x, \bar{Y}_0^{\text{out}}(x))$ to $(1, \bar{Y}_0^{\text{out}}(1))$, *i.e.*,

$$\bar{Y}_0^{\text{out}}(u) = 1 - u + x_* \ln u \quad (\text{A.2.2a})$$

$$\simeq \bar{Y}_0^{\text{out}}(x) + \frac{\bar{Y}_0^{\text{out}}(1) - \bar{Y}_0^{\text{out}}(x)}{1 - x} (u - x) \quad (\text{A.2.2b})$$

343

$$= Y_0^{\text{out}}(x) - \frac{Y_0^{\text{out}}(x)}{1-x}(u-x) \tag{A.2.2c}$$

344
345

We need to evaluate $Y_0^{\text{out}}(x)$ at its maximum point, namely $x = x_*$, hence the relevant approximation is [cf. Equation (10)]

346

$$Y_0^{\text{out}}(u) \simeq \bar{y}_0 - \frac{\bar{y}_0}{1-x_*}(u-x_*) = \bar{y}_0 \frac{1-u}{1-x_*} = \frac{1-x_*(1-\ln x_*)}{1-x_*}(1-u). \tag{A.2.3}$$

347
348

Inserting Equation (A.2.3) in Equation (A.2.1), where factors of $(1-u)$ in the numerator and denominator of the integrand now cancel out, we obtain

349

$$\mathcal{Y}_{\text{max}} \simeq \left(\frac{1-x_*}{1-x_*(1-\ln x_*)} \right) \int_{x_*}^1 \left(\frac{x_*}{u^2} - \frac{1}{u} \right) du = \left(\frac{1-x_*}{1-x_*(1-\ln x_*)} \right) (1-x_* + \ln x_*), \tag{A.2.4}$$

350

which yields Equation (25).

351

B Domain of Applicability of the First Order Approximation

352
353
354
355
356
357

We observed in [10] that for sufficiently large values of \mathcal{R}_0 , x_f is $\mathcal{O}(\epsilon)$. In this limit, the higher-order corrections in the first order left corner layer approximation (39) cause it to extend into an $\mathcal{O}(\epsilon)$ -strip in the biologically meaningless half-plane $x < 0$; consequently, for sufficiently large \mathcal{R}_0 , $Y^\uparrow(x; \epsilon)$ (40) fails to approximate the true trajectory $Y(x)$. Here, we compute an upper bound $\bar{\epsilon} = \bar{\epsilon}(\mathcal{R}_0)$ such that the corner solution remains in the biological right half plane for $\epsilon < \bar{\epsilon}$, and thus $(0, \bar{\epsilon})$ provides the domain of applicability of $Y^\uparrow(x; \epsilon)$.

358
359

Substituting C_0^{cor} (36), $C_{\text{ln}}^{\text{cor}}$ (37), and C_1^{cor} (38) into $X(y; \epsilon)$ [Table 1] gives us the matched first order left corner layer solution as a function of y :

$$\overset{\text{lc}}{X}(y; \epsilon) = x_f + \left(\frac{x_f}{x_* - x_f} \right) y - \epsilon \left(\frac{1-x_f}{x_* - x_f} \right) \left[\ln y - \ln \left(\left(\frac{1}{x_f} - 1 \right) (x_* - x_f) \right) - \left(\frac{1}{x_f} - 1 \right)^{-1} \mathcal{Y}_{x_f}^1(1) \right]. \tag{B.0.1}$$

360

Solving $\frac{d}{dy} \overset{\text{lc}}{X}(y; \epsilon) = 0$, we find that the minimum value of $\overset{\text{lc}}{X}(y; \epsilon)$, \underline{x}_1 , occurs at $y = \epsilon \left(\frac{1}{x_f} - 1 \right)$:

361

$$\underline{x}_1 = \overset{\text{lc}}{X} \left(\epsilon \left(\frac{1}{x_f} - 1 \right); \epsilon \right) = x_f + \epsilon \ln \epsilon^{-1} \left(\frac{1-x_f}{x_* - x_f} \right) + \epsilon \left(\frac{1-x_f}{x_* - x_f} \right) \left[1 + \ln(x_* - x_f) + \left(\frac{1}{x_f} - 1 \right)^{-1} \mathcal{Y}_{x_f}^1(1) \right]. \tag{B.0.2}$$

362
363
364
365

(Similarly, we can obtain the right corner solution as a function of y , $\overset{\text{rc}}{X}(y; \epsilon)$; evaluating the latter at $y = \epsilon \left(\frac{1}{x_{i,2}} - 1 \right)$ gives an approximation to the maximum fraction susceptible, \bar{x}_1 . See Table 2). Proceeding as in §3.3, we may use the Lambert W function to convert the inequality $\underline{x}_1 > 0$ into an inequality for ϵ . We find $\underline{x}_1 > 0$ if and only if

$$\epsilon < \bar{\epsilon} = \frac{x_* - x_f}{\left(\frac{1}{x_f} - 1 \right) W_0 \left(\left(\frac{1}{x_f} - 1 \right)^{-1} e^{-\left(\frac{1}{x_f} - 1 \right)^{-1} \mathcal{Y}_{x_f}^1(1) - 1} \right)}. \tag{B.0.3}$$

Quantity		Expression	Equation
Equilibrium susceptible density	x_*	$\frac{1}{\mathcal{R}_0}$	(3)
Final size (KM)	x_f	$-x_* W_0(\mathcal{E}(-1/x_*))$	(9)
Peak prevalence (KM)	\bar{y}_0	$1 - x_*(1 - \ln(x_*))$	(10)
Effective initial condition	$x_{i,2}$	$1 + (1 - x_*) W_0\left(\mathcal{E}\left(-\frac{1-x_f}{1-x_*}\right)\right)$	(12)
Peak prevalence ($\epsilon > 0$)	\bar{y}_1	$\bar{y}_0 - \epsilon \frac{(1-x_*)(1-x_* + \ln x_*)}{1-x_*(1-\ln x_*)}$	(25)
Minimum prevalence	\underline{y}_1	$\left(\frac{1}{x_f} - 1\right) (x_* - x_f) x_f^{\frac{x_* - x_f + x_* x_f}{(1-x_f)(1-x_*)}} \left(\frac{1-x_f}{1-x_*}\right)^{\frac{1-x_*}{\epsilon}} e^{-\frac{x_* - x_f}{\epsilon} - \frac{x_*}{x_* - x_f}}$	(51)
Minimum susceptible density	\underline{x}_1	$x_f + \epsilon \left(\frac{1-x_f}{x_* - x_f}\right) \left[\ln \epsilon^{-1} + 1 + \ln(x_* - x_f) + \frac{x_* - x_f + x_* x_f}{(1-x_f)(1-x_*)} \ln x_f - \frac{x_*}{x_* - x_f} \right]$	(B.0.2)
Maximum susceptible density	\bar{x}_1	$x_{i,2} + \epsilon \frac{1-x_{i,2}}{x_{i,2} - x_*} \left[\ln \left(\frac{\epsilon \left(\frac{1}{x_{i,2}} - 1\right)}{\left(\frac{1}{x_f} - 1\right)(x_* - x_f)} \right) - \frac{x_* - x_f + x_* x_f}{(1-x_f)(1-x_*)} \ln x_f - \frac{x_*}{x_* - x_f} \right]$	—

Table 2: Approximations of quantities of epidemiological interest for disease invasions, *i.e.*, on the trajectory that emanates from the disease-free equilibrium (DFE), $(x_i, y_i) = (1, 0)$. Each entry may depend upon entries above it in the table (but never on entries below). These quantities are used in our approximations to the full trajectories in Table 3. We use “(KM)” to indicate quantities that are exact for the Kermack-McKendrick SIR model *without* vital dynamics ($\epsilon = 0$). With vital dynamics ($\epsilon > 0$), the peak prevalence \bar{y}_0 is an approximation, and there is no “final” size, but the quantity x_f appears in the approximation to the minimum fraction susceptible (\underline{x}_1). The expression for \underline{x}_1 is valid provided $\epsilon < \bar{\epsilon}$ Equation (B.0.3). We write the formulae for \underline{x}_1 and \bar{x}_1 as compactly as possible here; see Equation (B.0.2) for \underline{x}_1 written out with separate terms for each asymptotic order.

Solution	Notation	Expression	Branch	Domain	Equation
KM	$\bar{Y}_0^{\text{out}}(x, x_i)$	$x_i - x + x_* \ln\left(\frac{x}{x_i}\right)$	–	$[x_f, x_i]$	(8)
Outer	$\bar{Y}^{\text{out}}(x; \epsilon)$	$\bar{Y}_0^{\text{out}}(x, x_i) - \epsilon \mathcal{Y}_x^1(1) + \epsilon \left(\frac{1}{x_f} - 1\right) \ln \frac{x-x_f}{1-x_f}$	–	$[x_f, x_i]$	(23)
x -axis bdry	$Y^{\text{xb}}(x; \epsilon)$	$\left(\frac{1}{x_f} - 1\right) (x_* - x_f) \left(\frac{1-x_f}{1-x}\right)^{\frac{1-x_*}{\epsilon}} \frac{x_* - x_f + x_* x_f}{(1-x_f)(1-x_*)} e^{-\frac{x-x_f}{\epsilon} - \frac{x_*}{x_* - x_f}}$	–	$[x_f, x_*]$	(47)
Left corner	$Y^{\text{lc}i}(x; \epsilon)$	$-\epsilon \left(\frac{1}{x_f} - 1\right) W_i \left(-\frac{x_* - x_f}{\epsilon} x_f^{\frac{x_* - x_f + x_* x_f}{(1-x_f)(1-x_*)}} e^{-\frac{x-x_f}{\epsilon} \frac{x_* - x_f}{1-x_f} - \frac{x_*}{x_* - x_f}} \right)$	$i = \begin{cases} -1 & \text{above} \\ 0 & \text{below} \end{cases}$	$[x_f, x_*]$	(39)
Right corner	$Y^{\text{rc}i}(x; \epsilon)$	$-\epsilon \left(\frac{1}{x_{i,2}} - 1\right) W_i \left(-\frac{\left(\frac{1}{x_f} - 1\right)(x_* - x_f)}{\epsilon \left(\frac{1}{x_{i,2}} - 1\right)} x_f^{\frac{x_* - x_f + x_* x_f}{(1-x_f)(1-x_*)}} e^{-\frac{x_{i,2} - x}{\epsilon} \frac{x_{i,2} - x_*}{1-x_{i,2}} - \frac{x_*}{x_* - x_f}} \right)$	$i = \begin{cases} -1 & \text{above} \\ 0 & \text{below} \end{cases}$	$[x_*, x_{i,2}]$	(49)
Matched, above	$Y^\dagger(x; \epsilon)$	$\bar{Y}_0^{\text{out}}(x, x_i) + Y^{\text{lc}i}(x; \epsilon) - \left(\frac{x_*}{x_f} - 1\right) (x - x_f) + \epsilon \mathcal{Y}_{x_f}^1(1)$	–	$[x_f, x_i]$	(40)
Matched, below	$Y_\downarrow(x; \epsilon)$	$Y^{\text{xb}}(x; \epsilon) + Y^{\text{lc}i}(x; \epsilon) + Y^{\text{rc}i}(x; \epsilon) - \left(\frac{1}{x_f} - 1\right) (x_* - x_f) x_f^{\frac{x_* - x_f + x_* x_f}{(1-x_f)(1-x_*)}} e^{-\frac{x_*}{x_* - x_f} \left(e^{-\frac{x-x_f}{\epsilon} \frac{x_* - x_f}{1-x_f}} + e^{-\frac{x_{i,2} - x}{\epsilon} \frac{x_{i,2} - x_*}{1-x_{i,2}}} \right)}$	–	$[x_f, x_{i,2}]$	(50)

Table 3: First order matched approximations to the initial epidemic following disease invasion $[(x_i, y_i) = (1, 0)]$. See Table 2 for x_* , x_f , and $x_{i,2}$ expressed in terms of \mathcal{R}_0 and ϵ . Equation (18) defines $\mathcal{Y}_a^b(1) = \int_a^b \left[\left(\frac{1}{u} - 1\right) \left(\frac{x_*}{u} - 1\right) / \bar{Y}_0^{\text{out}}(u, x_i) - \left(\frac{1}{x_f} - 1\right) \frac{1}{u-x_f} \right] du$. We use (52) to approximate $\mathcal{Y}_{x_f}^1(1)$ analytically. Above and below indicate solutions that are valid above and below the x nullcline, $y = \epsilon \left(\frac{1}{x} - 1\right)$. The expression for $Y^{\text{rc}i}(x; \epsilon)$, and thus the matched solutions $Y^\dagger(x; \epsilon)$ and $Y_\downarrow(x; \epsilon)$ are valid provided $\epsilon < \bar{\epsilon}$ Equation (B.0.3).

Constant	Expression	Equation
C_0^{out}	$y_i + x_i - x_* \ln x_i$	(7)
C_1^{out}	$-\mathcal{Y}_{x_*}^1(1) - \left(\frac{1}{x_f} - 1\right) \ln\left(\frac{1-x_f}{x_*-x_f}\right)$	(22)
C_0^{cor} (left)	x_f	(36)
C_{\ln}^{cor} (left)	$-\frac{1-x_f}{x_*-x_f}$	(37)
C_1^{cor} (left)	$\frac{1-x_f}{x_*-x_f} \left[\ln\left(\left(\frac{1}{x_f} - 1\right)(x_* - x_f)\right) + \left(\frac{1}{x_f} - 1\right)^{-1} \mathcal{Y}_{x_f}^1(1) \right]$	(38)
c_0^ϕ	x_f	(44)
C_0^ϕ	$x_f - (1 - x_*) \ln(1 - x_f)$	(45)
C_1^ϕ	$\ln\left[\left(\frac{1}{x_f} - 1\right)(x_* - x_f)\right] + \left(\frac{1}{x_f} - 1\right)^{-1} \mathcal{Y}_{x_f}^1(1)$	(46)
C_0^{cor} (right)	$x_{i,2}$	–
C_{\ln}^{cor} (right)	$\frac{1-x_{i,2}}{x_{i,2}-x_*}$	–
C_1^{cor} (right)	$-\frac{1-x_{i,2}}{x_{i,2}-x_*} \left[\ln\left[\left(\frac{1}{x_f} - 1\right)(x_* - x_f)\right] + \left(\frac{1}{x_f} - 1\right)^{-1} \mathcal{Y}_{x_f}^1(1) \right]$	–
C_0^{out} (2 nd)	$x_{i,2} - x_* \ln x_{i,2}$	–
C_1^{out} (2 nd)	$-\left(\frac{1}{x_{f,2}} - 1\right) \ln\left(\frac{\left(\frac{1}{x_f} - 1\right)(x_* - x_f)(1 - x_{i,2})}{\left(\frac{1}{x_{i,2}} - 1\right)(x_{i,2} - x_*)(x_{i,2} - x_{f,2})}\right) + \frac{\frac{1}{x_{f,2}} - 1}{\frac{1}{x_f} - 1} \mathcal{Y}_{x_f}^1(1) - \mathcal{Y}_{x_*}^{x_{i,2}}(x_{i,2})$	(56)
C_0^{cor} (left, 2 nd)	$x_{f,2}$	–
C_{\ln}^{cor} (left, 2 nd)	$-\frac{1-x_{f,2}}{x_*-x_{f,2}}$	–
C_1^{cor} (left, 2 nd)	$\frac{1-x_{f,2}}{x_*-x_{f,2}} \left[\left(\frac{1}{x_{f,2}} - 1\right)^{-1} \mathcal{Y}_{x_{f,2}}^{x_{i,2}}(x_{i,2}) - \frac{\frac{1}{x_{i,2}} - 1}{\left(\frac{1}{x_f} - 1\right)\left(\frac{1}{x_{f,2}} - 1\right)} \mathcal{Y}_{x_f}^1(1) + \frac{\frac{1}{x_{i,2}} - 1}{\frac{1}{x_{f,2}} - 1} \ln\left(\frac{\left(\frac{1}{x_f} - 1\right)(x_* - x_f)(1 - x_{i,2})}{\left(\frac{1}{x_{i,2}} - 1\right)(x_{i,2} - x_*)(x_{i,2} - x_{f,2})}\right) + \ln\left(\frac{\left(\frac{1}{x_{f,2}} - 1\right)(x_* - x_{f,2})(x_{i,2} - x_{f,2})}{1 - x_{f,2}}\right) \right]$	–

Table 4: First order matching constants for disease invasions $[(x_i, y_i) = (1, 0)]$. Left and right indicate constants appearing in the left and right corner solutions, while 2nd indicates constants for the second epidemic wave. See Table 2 for x_* , x_f , and $x_{i,2}$ expressed in terms of \mathcal{R}_0 and ϵ . The final expressions with these values for the matching constants are listed in Table 3.

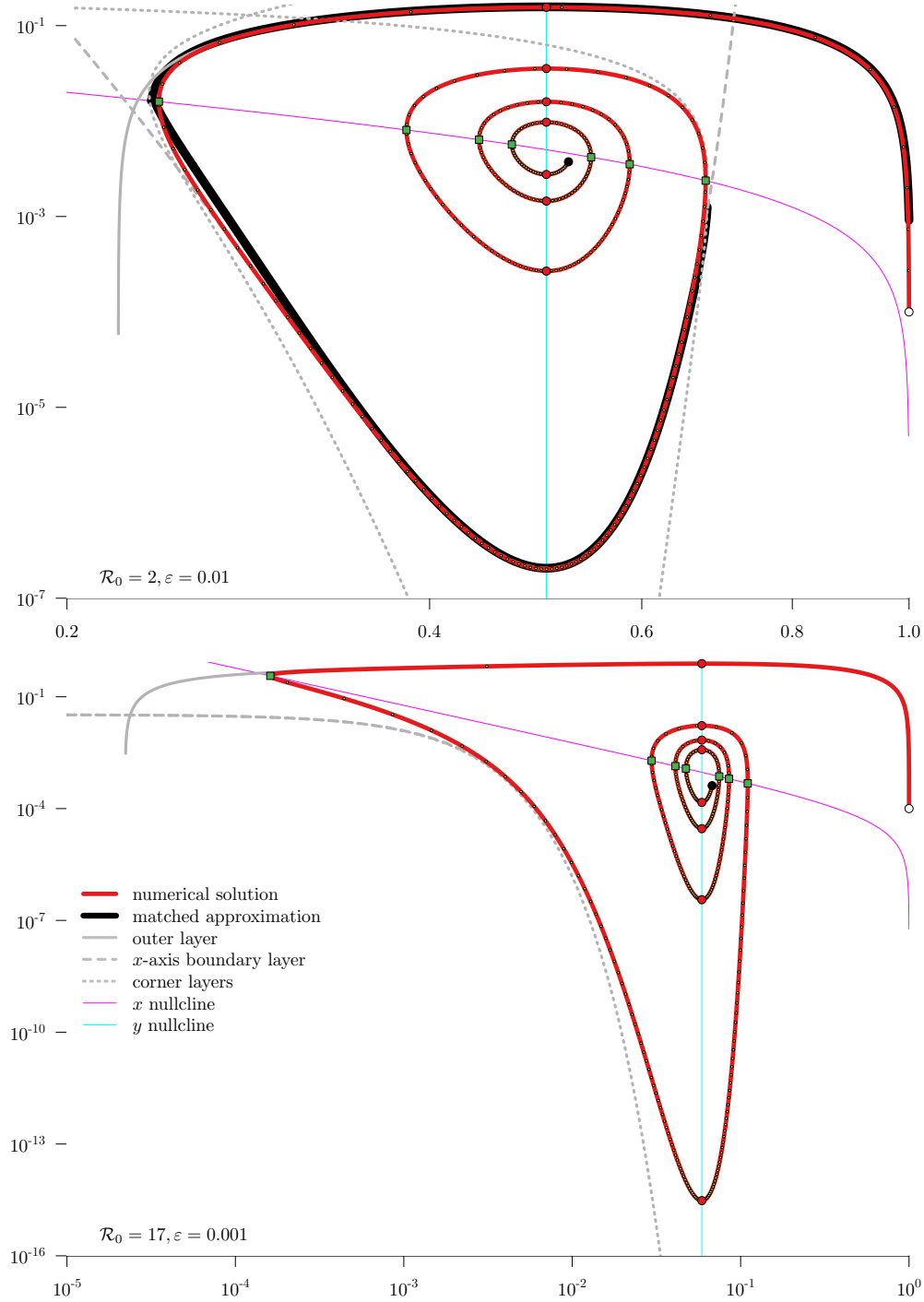


Figure 2: Solutions of the SIR ODEs Equation (4) and first order approximations (Table 3). This figure should be compared with the zeroth order approximations shown in [10, Figures 4 and 5]. *Top panel:* $\mathcal{R}_0 = 2$, $\varepsilon = 0.01$. *Bottom panel:* $\mathcal{R}_0 = 17$, $\varepsilon = 0.001$; similar to measles and whooping cough [10, Table 1]. Various outer and inner approximations are shown in grey, and the matched approximation is black. Numerically computed solutions to Equation (4) are red. In the bottom panel, the matched solution is not shown because matching fails for this parameter combination ($5.9 \times 10^{-5} = \varepsilon > \bar{\varepsilon} \approx 5.7 \times 10^{-9}$; cf. Equation (B.0.3)). Nevertheless, the local solutions that we show still provide accurate approximations, with the exception of the corner layer solution that fails and prevents successful matching.

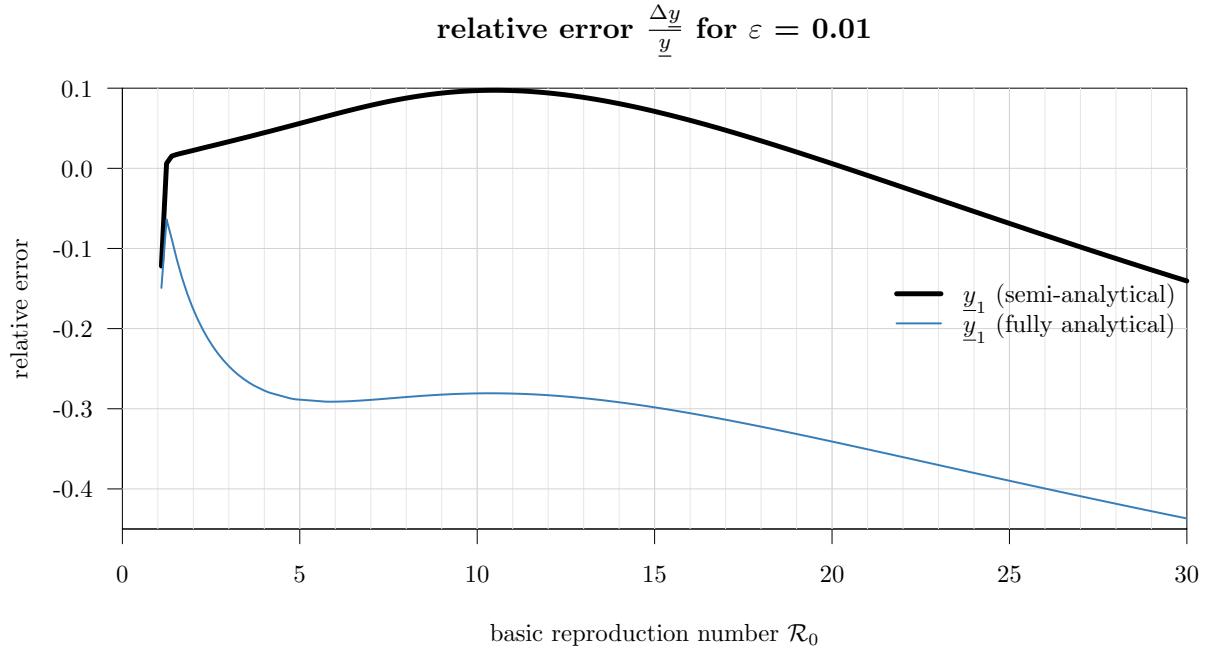
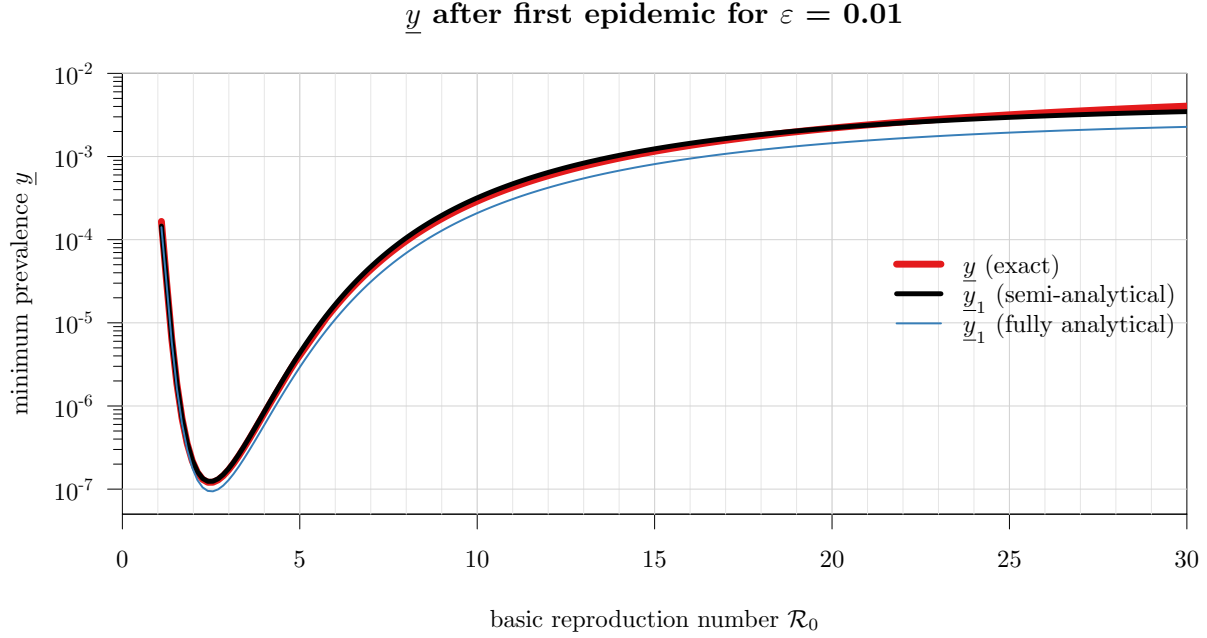
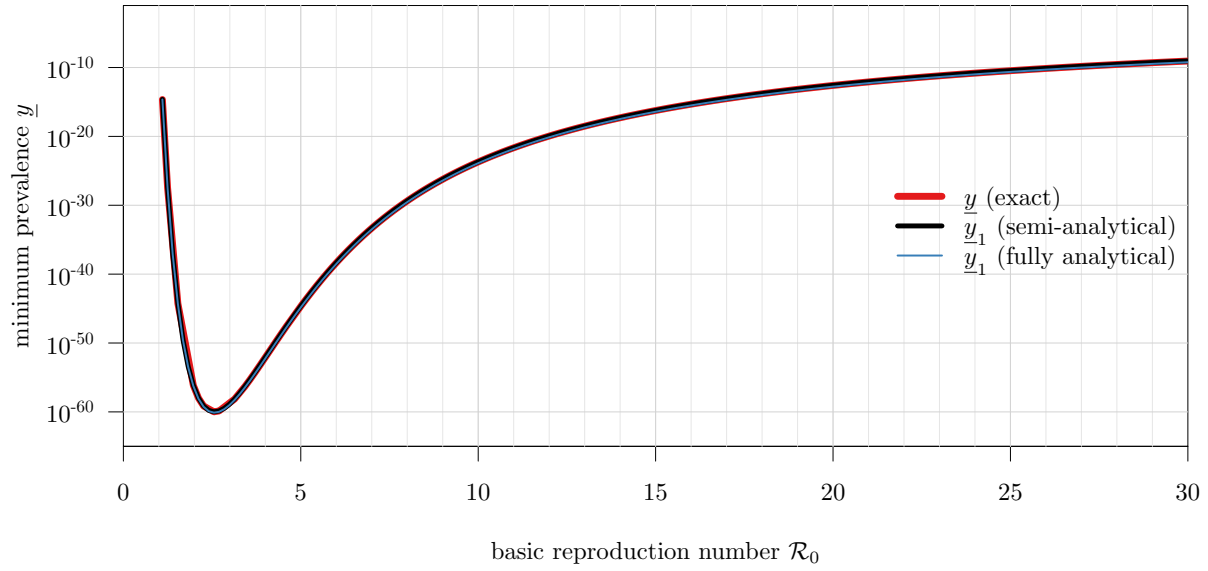


Figure 3: Minimum prevalence following an initial epidemic, as a function of \mathcal{R}_0 for $\varepsilon = 0.01$. *Top panel:* minimum prevalence \underline{y} from “exact” numerical solution of Equation (4); from our semi-analytical approximation \underline{y}_1 (51, which depends on computing the integral $\mathcal{Y}_{x_f}^1(1)$ numerically); and from our fully analytical closed-form approximation to \underline{y}_1 (obtained using Equation (52)). *Bottom panel:* Relative errors when approximating \underline{y} using the semi-analytical \underline{y}_1 Equation (51), and the fully analytical approximate \underline{y}_1 .

\underline{y} after first epidemic for $\varepsilon = 0.001$



relative error $\frac{\Delta y}{\underline{y}}$ for $\varepsilon = 0.001$

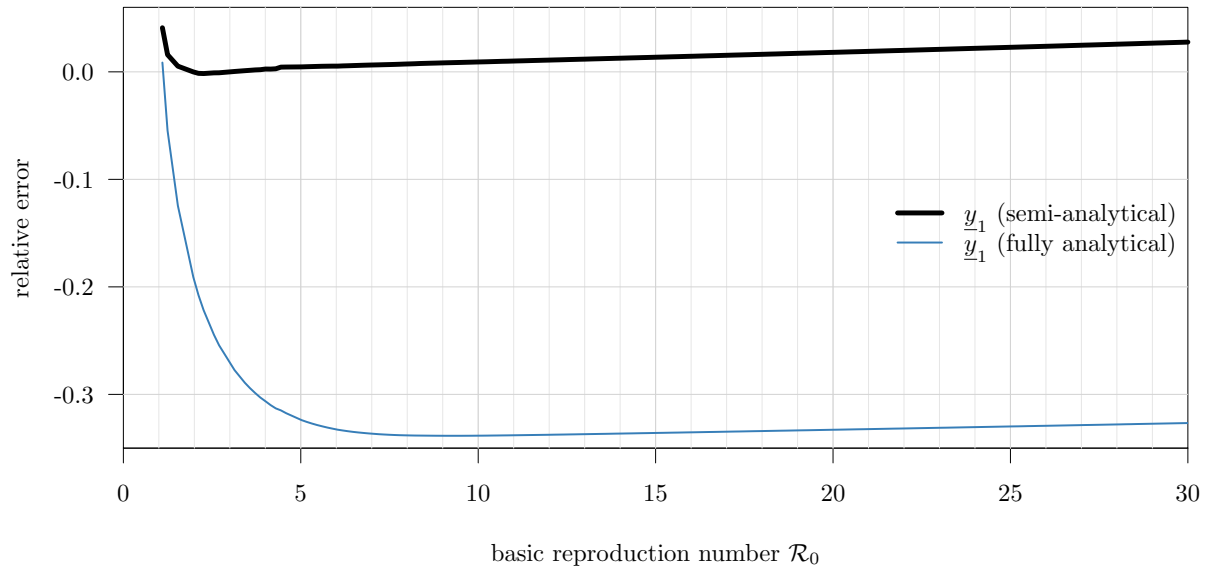
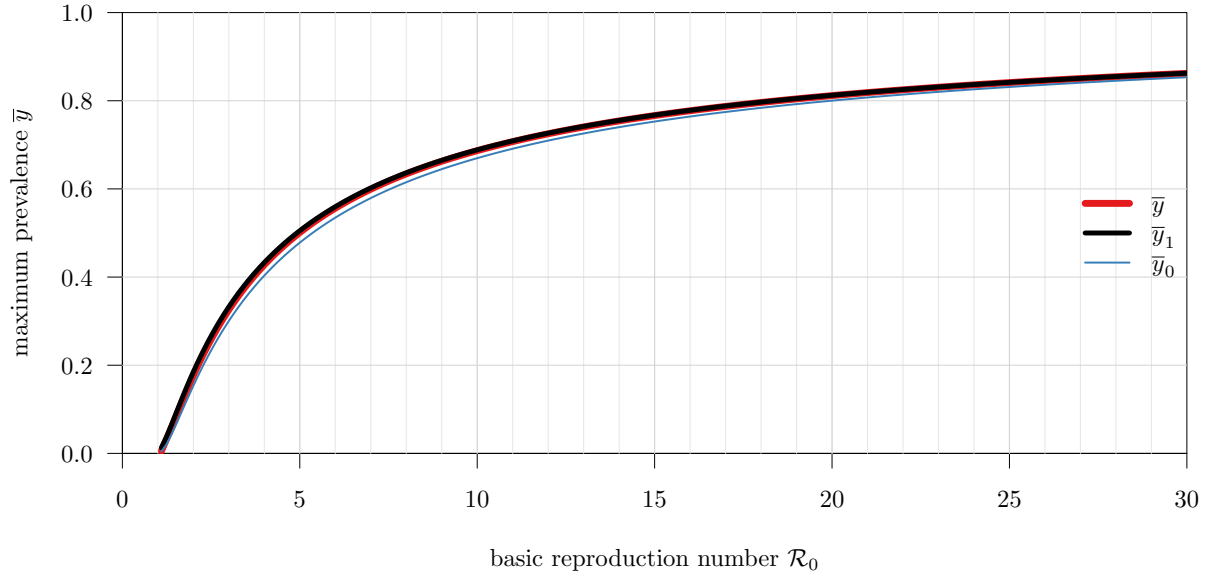


Figure 4: Minimum prevalence after a first epidemic. Like Figure 3 but for $\varepsilon = 0.001$.

\bar{y} during first epidemic for $\varepsilon = 0.1$



relative error $\left| \frac{\Delta \bar{y}}{\bar{y}} \right|$ for $\varepsilon = 0.1$

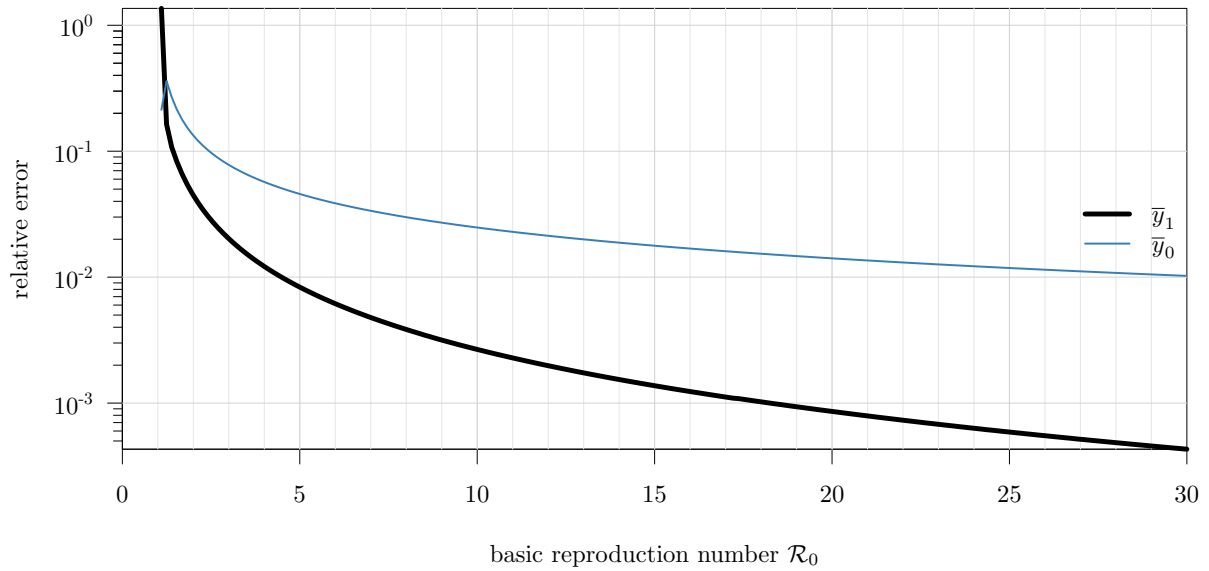
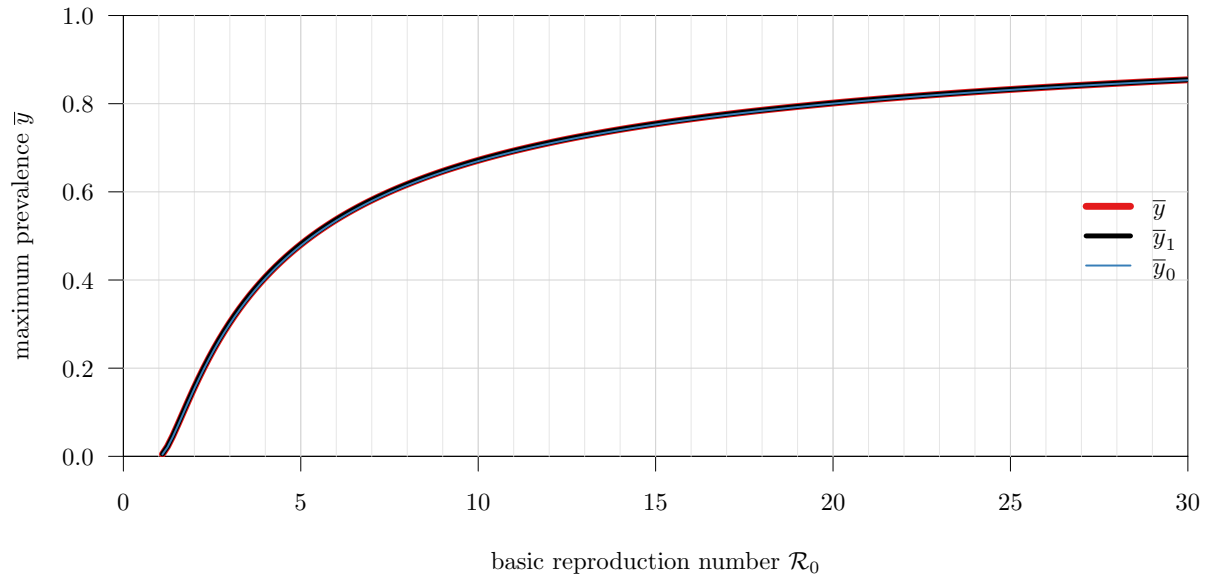


Figure 5: Maximum prevalence. Like Figure 3 but for \bar{y} with $\varepsilon = 0.1$, and using a logarithmic scale in the bottom panel.

\bar{y} during first epidemic for $\varepsilon = 0.01$



relative error $\left| \frac{\Delta \bar{y}}{\bar{y}} \right|$ for $\varepsilon = 0.01$

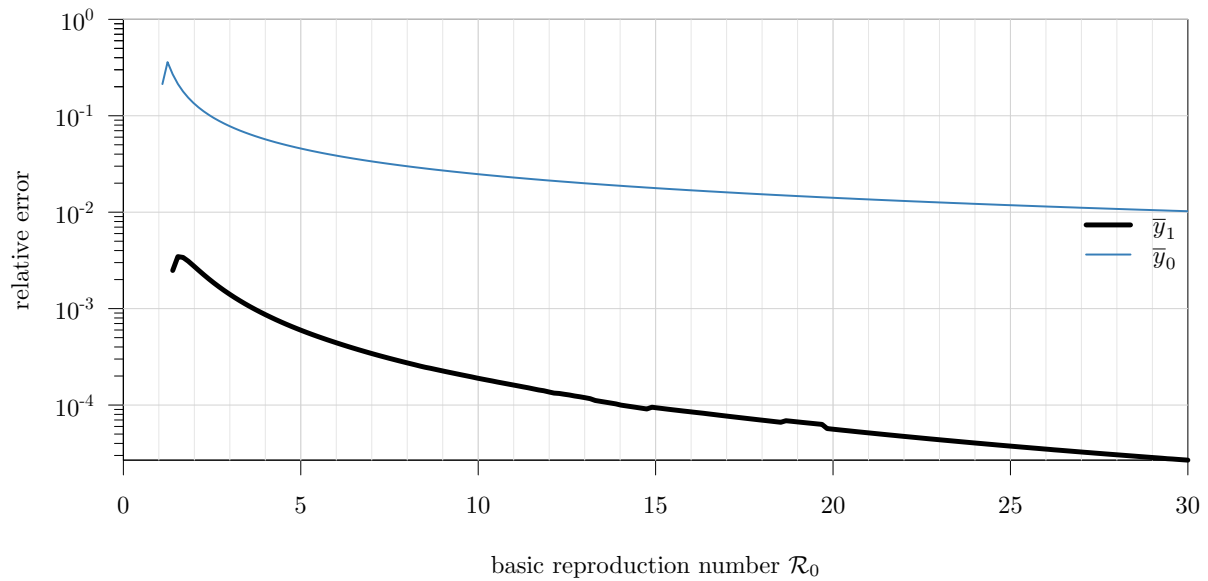


Figure 6: Maximum prevalence. Like Figure 5 but for $\varepsilon = 0.01$.